

# Microburst Scale Size Derived from Multiple Bounces of a Microburst Simultaneously Observed with the FIREBIRD-II CubeSats

Mykhaylo Shumko<sup>1</sup>, John Sample<sup>1</sup>, Arlo Johnson<sup>1</sup>, Bern Blake<sup>2</sup>, Alex Crew<sup>3</sup>, Harlan Spence<sup>4</sup>, David Klumpar<sup>1</sup>, Oleksiy Agapitov<sup>5</sup>, Matthew Handley<sup>1</sup>

<sup>1</sup>Department of Physics, Montana State University, Bozeman, Montana, USA

<sup>2</sup>Space Science Applications Laboratory, The Aerospace Corporation, Los Angeles, California, USA

<sup>3</sup>The Johns Hopkins University Applied Physics Laboratory LLC, Laurel, Maryland, USA

<sup>4</sup>Institute for the Study of Earth, Oceans, and Space, University of New Hampshire, Durham, New Hampshire, USA

<sup>5</sup>Space Sciences Laboratory, UC Berkeley, Berkeley, California, USA

## Key Points:

- The lower bounds on the microburst scale size at LEO were  $29 \pm 1$  km (latitudinal) and  $51 \pm 11$  km (longitudinal).
- Deduced lower bound equatorial scale size was similar to the whistler-mode chorus source scale.

## Abstract


We present the observation of a spatially large microburst with multiple bounces made simultaneously by the FIREBIRD-II CubeSats on February 2nd, 2015. This is the first observation of a microburst with a subsequent decay made by two co-orbiting but spatially separated spacecraft. From these unique measurements, we place estimates on the lower bounds of the spatial scales as well as quantify the electron bounce periods. Its lower bound latitudinal scale size was  $29 \pm 1$  km and the longitudinal scale size was  $51 \pm 11$  km in low earth orbit. We mapped these scale sizes to the magnetic equator and found that the radial and azimuthal scale sizes were at least  $504 \pm 14$  km and  $530 \pm 119$  km, respectively. These lower bound equatorial scale sizes are similar to whistler-mode chorus wave source scale sizes, which supports the hypothesis that microbursts are a product of electron scattering by chorus waves. Lastly, we estimated the bounce periods for 200-800 keV electrons and found good agreement with four common magnetic field models.

## 1 Introduction

The dynamics of radiation belt electrons are complex, and are driven by competition between source and loss processes. A few possible loss processes are radial diffusion [Shprits and Thorne, 2004], magnetopause shadowing [Ukhorskiy et al., 2006], and pitch angle and energy diffusion due to scattering of electrons by plasma waves [e.g. Abel and Thorne, 1998; Summers et al., 1998; Meredith et al., 2002; Selesnick et al., 2003; Horne and Thorne, 2003; Thorne et al., 2005; Mozer et al., 2018]. There are a variety of waves that cause pitch angle scattering, including electromagnetic ion cyclotron waves, plasmaspheric hiss, and chorus [Millan and Thorne, 2007; Thorne, 2010]. Chorus predominantly occurs in the dawn sector (6-12 magnetic local times (MLT)) [Li et al., 2009] where it accelerates electrons with large equatorial pitch angles and scatters electrons with small equatorial pitch angles [Horne and Thorne, 2003]. Some of these electrons may be impulsively scattered into the loss cone, where they result in short-duration ( $\sim 100$  ms) enhancements in precipitating flux called microbursts.


Anderson and Milton [1964] coined the term microburst to describe high altitude balloon observations of  $\sim 100$  ms duration enhancements of bremsstrahlung X-rays emitted from scattered microburst electrons impacting the atmosphere. Since then, non-relativistic ( $< \sim 500$  keV) microbursts have been routinely observed with other balloon missions [Parks, 1967; Woodger et al., 2015; Anderson et al., 2017]. Relativistic microbursts have not yet been observed by high altitude balloons in the dawn sector with the following evidence. Millan et al. [2002] and Woodger et al. [2015] discuss balloon observations of longer-duration relativistic duskside precipitation and non-relativistic microbursts, but do not provide any observational evidence of relativistic microbursts in their balloon data. This lack of observation may be explained by relatively weaker pitch angle scattering of relativistic electrons by chorus [Lee et al., 2012].

In addition to the X-ray signature proxy for bursts of electron precipitation, the precipitating relativistic and non-relativistic electrons have been measured in situ by spacecraft orbiting in low earth orbit (LEO). Hereinafter, we refer to these electron signatures observed by LEO spacecraft also as microbursts. Microbursts have been observed with, e.g. the Solar Anomalous and Magnetospheric Particle Explorer (SAMPEX)  $> 150$  keV and  $> 1$  MeV channels [Nakamura et al., 1995, 2000; Blake et al., 1996; Lorentzen et al., 2001a,b; O'Brien et al., 2003, 2004; Blum et al., 2015] and Focused Investigation of Relativistic Electron Bursts: Intensity, Range, and Dynamics (FIREBIRD-II) with its  $> 200$  keV energy channels [Crew et al., 2016; Anderson et al., 2017; Breneman et al., 2017]. To characterize the source of microbursts, Lorentzen et al. [2001b] found that microbursts and chorus waves predominantly occur in the dawn sector and Breneman et al. [2017] made a direct observational link between individual microbursts and chorus elements.

Understanding  microburst precipitation is important to radiation belt dynamics since microbursts have been modeled and empirically estimated to be capable of depleting the relativistic electron population in the outer radiation belt on the order of a day [O'Brien *et al.*, 2004; Thorne *et al.*, 2005; Shprits *et al.*, 2007; Breneman *et al.*, 2017]. An important parameter in this estimation of instantaneous radiation belt electron losses due to microbursts is their scale size. Parks [1967] used balloon measurements of bremsstrahlung X-rays to estimate the high altitude scale size of predominantly low energy microbursts to be  $40 \pm 14$  km. In Blake *et al.* [1996] a microburst with multiple bounces was observed by SAMPEX, and the microburst's latitudinal scale size in LEO was estimated to have been "at least a few tens of kilometers". Blake *et al.* [1996] concluded that typically microbursts are less than a few tens of electron gyroradii in size (at  $L = 5$  at LEO, the gyroradii of 1 MeV electrons is on the order of 100 m). Dietrich *et al.* [2010] used SAMPEX along with ground-based very low frequency stations to conclude that during one SAMPEX pass, the observed microbursts had scale sizes less than 4 km.

Since February 1st, 2015, microbursts have been observed by FIREBIRD-II, a pair of CubeSats in LEO. Soon after launch, when the two FIREBIRD-II spacecraft were at close range, a microburst with a scale size greater than 11 km was observed [Crew *et al.*, 2016]. On the same day, FIREBIRD-II simultaneously observed a microburst with multiple bounces. The microburst decay was observed over a period of a few seconds, while the spacecraft were traveling predominantly in latitude. Here we present the analysis and results of the latitude and longitude scale sizes and bounce periods of the first microburst with multiple bounces observed with the two FIREBIRD-II spacecraft.

## 2 Spacecraft and Observation

The FIREBIRD missions are comprised of a pair of identically-instrumented 1.5U CubeSats (15 x 10 x 10 cm) that are designed to measure electron precipitation in LEO [Spence *et al.*, 2012; Klumpar *et al.*, 2015]. The second mission, termed FIREBIRD-II, was launched on January 31st 2015. The two FIREBIRD-II CubeSats, identified as Flight Unit 3 (FU3) and Flight Unit 4 (FU4), were placed 632 km apogee, 433 km perigee, and  $99^\circ$  inclination orbit [Crew *et al.*, 2016]. FU3 and FU4 are orbiting in a string of pearls  configuration with FU4 ahead, to resolve the space-time ambiguity of events that are either spatial or temporal. Each FIREBIRD-II unit has two solid state detectors: one is mounted essentially at the spacecraft surface, covered only by a thin foil acting as a sun shade, with a field of view of  $90^\circ$  (surface detector), and the other is beneath a collimator which restricts the field of view to  $54^\circ$  (collimated detector). Only FU3 has a functioning surface detector, so this analysis utilizes the collimated detectors. FU3's surface and collimated detectors, as well as FU4's collimated detector observe electron fluxes in six energy channels from  $\sim 230$  keV to  $> 1$  MeV, with an adjustable sampling rate of 18.75 ms by default and as fast as 12.5 ms.

On February 2nd, 2015 at 06:12 UT, both FIREBIRD-II spacecraft simultaneously observed an initial microburst, followed by subsequent periodic electron enhancements of diminishing amplitude. This is thought to be the signature of a single burst of electrons, some of which precipitate, but the rest mirror near the spacecraft then bounce off the mirror in the conjugate hemisphere to produce a train of decaying peaks. This bounce signature occurred during the transition between the main and recovery phases of a storm with a minimum Dst of -44 nT ( $K_p = 4$ , and  $AE \approx 400$  nT). Figure 1 shows the High Resolution (HiRes) microburst electron flux, sampled at 18.75 ms. Five peaks were observed by both spacecraft. The fifth peak observed by FU4 was comparable to the Poisson noise and was not used in this analysis. This microburst was observed from the first energy channel ( $\approx 200 - 300$  keV), to the fourth energy channel ( $\approx 500 - 700$  keV), and FU3's surface detector observed the microburst up to the fifth energy channel (683 - 950 keV).

The HiRes data in Fig. 1 shows signs of energy dispersion, characterized by higher energy electrons arriving earlier than the lower energies. This time of flight energy dispersion

tends to smear out the initial sharp burst upon each subsequent bounce. The first peak does not appear to be dispersed, and subsequent peaks show dispersion consistent across energy channels. The black vertical bars have been added to Fig. 1 to highlight this energy dispersion. This dispersion signature and amplitude decay implies that the first peak was observed soon after the electrons were scattered, followed by decaying bounces.

At this time, in magnetic coordinates, FIREBIRD-II was at McIlwain  $L = 4.7$  and  $MLT = 8.3$ , calculated with the Tsyganenko 1989 (T89) magnetic field model [Tsyganenko, 1989]. Geographically, they were above Sweden, latitude =  $63^\circ\text{N}$ , longitude =  $15^\circ\text{E}$ , altitude = 650 km. This location is critical for our analysis. This geographic location is magnetically conjugate to the east of the so-called South Atlantic Anomaly (SAA). The SAA is the location where the mirror points of electrons tend to occur at locations deeper in the atmosphere owing to the offset of the dipole magnetic field from the Earth's center. Electrons that encounter the SAA are removed from their eastward longitudinal drift paths. This loss effect is termed the drift loss cone (DLC). Precipitation loss that occurs to the east of the SAA is outside the region where drift loss is strong and so is termed the bounce loss cone (BLC). FU3 and FU4 are therefore both in regions that are unaffected by DLC effects, and so are optimally able to see details of only BLC effects. Indeed, locally mirroring electrons would have mirrored at 95 km in the opposite hemisphere, calculated with T89 and IRBEM-Lib [Boscher *et al.*, 2012]. From the analysis done by Fang *et al.* [2010], the peak in the total ionization rate in the atmosphere for 100 keV electrons is around 80 km altitude, while the total ionization rate from 1 MeV electrons peaks around 60 km altitude. It is, therefore, expected that a fraction of the microburst electrons will survive each encounter with the atmosphere. By plotting the peak flux as a function of bounce (not shown), it was found that 40 - 60 % of the microburst electrons were lost on the first bounce, similar to the 33% loss per bounce observed for a bouncing microburst observed by SAMPEX [Thorne *et al.*, 2005].

### 3 Analysis

At the beginning of the FIREBIRD-II mission, two issues prevented the proper analysis of the microburst's spatial scale size: the spacecraft clocks were not synchronized, and their relative positions were not accurately known. We addressed these issues with a cross-correlation time lag analysis described in detail in the supporting information (SI). From this analysis, the time correction was  $2.28 \pm 0.12$  s (applied to Fig. 1) and the separation was  $19.9 \pm 0.9$  km at the time of the microburst observation.

#### 3.1 Electron Bounce Period

We used this unique observation of bouncing electrons to calculate the bounce period,  $t_b$ , as a function of energy and compare it to  $t_b$  derived from four magnetic field models. The observed  $t_b$  and uncertainties were calculated by fitting the baseline-subtracted HiRes flux. The baseline flux used in this analysis is given in O'Brien *et al.* [2004] as the flux at the 10th percentile over a specified time interval, which in this analysis was taken to be 0.5 seconds. The flux was fitted with a superposition of Gaussians for each energy channel, and the uncertainty in flux was calculated using the Poisson error from the microburst and baseline fluxes summed in quadrature. Using the fit parameters, the mean  $t_b$  for the lowest four energy channels is shown in Fig. 2. The trend of decreasing  $t_b$  as a function of energy is evident in Fig. 2, which further supports the assumption that the subsequent peaks are bounces, and not a train of microbursts scattered by bouncing chorus.

The decaying peaks in the 231-408 keV electron flux observed by FU3's lowest two energy channels (see Fig. 1) were right-skewed. This implies that there was in-channel energy dispersion within those channels that is smeared out by the broad energy channels. Since  $t_b$  of higher energy electrons is shorter, a right-skewed peak implies that higher energy electrons were more abundant within each channel. A Gaussian fit cannot account for this in-

channel dispersion, and as a first order correction, minima between peaks was used to calculate  $t_b$ , and is shown in Fig. 2.

To compare the observed and modeled  $t_b$ , we superposed  $t_b$  curves for various models including an analytical solution in a dipole [Schulz and Lanzerotti, 1974], and numerical models: T89, Tsyganenko 2004 (T04) [Tsyganenko and Sitnov, 2005], and Olson & Pfister Quiet [Olson and Pfister, 1982] in Fig. 2. The numerical  $t_b$  curves were calculated using a wrapper for IRBEM-Lib. This code traces the magnetic field line between mirror points, and calculates  $t_b$  assuming conservation of energy and the first adiabatic invariant for electrons mirroring at FIREBIRD-II. With the empirical  $t_b$ , the models agree within FIREBIRD-II's uncertainties, but the T04 model has the largest discrepancy compared to the other models.

### 3.2 Microburst Energy Spectra

Next, we investigated the energy spectra of this microburst. The energy spectra was modeled with an exponential that was fit to the peak flux derived from the Gaussian fit parameters in section 3.1 to all but the highest energy channel. We found that the E-folding energy,  $E_0 \sim 100$  keV. This spectra is similar to the spectra shown in Lee *et al.* [2005] who used STSAT-1 and Datta *et al.* [1997] who used a sounding rocket. The energy spectra is soft for a typical microburst observed with FIREBIRD-II. There was no statistically significant change in  $E_0$  for subsequent bounces which further supports a single bouncing packet over a train of isolated bursts.

### 3.3 Microburst Scale Sizes

Lastly, after we applied the corrections detailed in the SI, we mapped the locations of FU3 and FU4 in Fig. 3. The locations where FU3 saw peaks 1-5 and where FU4 saw peaks 1-4 are shown as P1-5 and P1-4, respectively. The lower bound on the latitudinal extent of the microburst was the difference in latitude between P1 on FU3 and P4 on FU4 and was found to be  $29 \pm 1$  km. The uncertainty was estimated from the spacecraft separation uncertainty described in the SI. This scale size is the largest reported by FIREBIRD-II.

To calculate the longitudinal scale size of the microburst, we assumed that the scattered electrons observed in the last bounce by FIREBIRD-II, must have drifted east from their initial scattering longitude. Following geometrical arguments, the distance that electrons drift east in a single bounce is a product of the circumference of the drift shell foot print, and the fraction of the total drift orbit traversed in a single bounce and is given by,

$$d_{az} = 2\pi(R_E + A) \cos(\lambda) \frac{t_b}{\langle T_d \rangle} \quad (1)$$

where  $R_E$  is the Earth's radius,  $A$  is the spacecraft altitude,  $\lambda$  is the magnetic latitude,  $t_b$  is the electron bounce period, and  $\langle T_d \rangle$  is the electron drift period. Parks [2003] derived  $\langle T_d \rangle$  to be,

$$\langle T_d \rangle \approx \begin{cases} 43.8/(L \cdot E) & \text{if } \alpha_0 = 90^\circ \\ 62.7/(L \cdot E) & \text{if } \alpha_0 = 0^\circ \end{cases} \quad (2)$$

where  $E$  is the electron energy in MeV,  $L$  is the L shell, and  $\alpha_0$  is the equatorial pitch angle. Electrons mirroring at FIREBIRD-II have  $\alpha_0 \approx 3.7^\circ$  and so the  $\alpha_0 = 0^\circ$  limit was used.

The microburst's longitudinal scale size is defined as the distance the highest energy electrons drifted in the time between the observations of the first and last peaks. This scale size is given by  $D_{az} = n d_{az}$  where  $n$  is the number of bounces observed. The stars with energy labels in Fig. 3 represent the locations of electrons with that energy when the microburst was observed at P1, and drifted eastward to be last seen at P5 for FU3 and P4 for FU4. The larger longitudinal scale size was observed by FU3 and is shown with the red dashed box in Fig. 3. The minimum scale size was  $39 \pm 9$  km for the 555 keV electrons and  $51 \pm 11$  km for the 771 keV electrons (lower and upper bound of the fourth energy channel).

The uncertainty was estimated by propagating the uncertainty in the spacecraft separation through Eq. 1.

To investigate how the microburst scale size relates to its generation mechanism near the magnetic equator, the microburst's longitudinal and latitudinal scale sizes and their uncertainties in LEO were mapped to the magnetic equator with T89. The radial scale size (latitudinal scale mapped from LEO) was greater than  $504 \pm 14$  km. The azimuthal scale size (longitudinal scale mapped from LEO) of 555 keV electrons was greater than  $451 \pm 103$  km and for the 771 keV electrons it was greater than  $530 \pm 119$  km.

#### 4 Discussion and Conclusions

We presented the first observation of a large microburst with multiple bounces made possible by the twin FIREBIRD-II CubeSats. The microburst's lower bound LEO latitudinal and longitudinal scale sizes of  $29 \pm 1$  km and  $51 \pm 11$  km make it one of the largest observed. The microburst's LEO scale size was larger than the latitudinal scale sizes of typical  $> 1$  MeV microbursts reported in *Blake et al.* [1996],  $\approx 10$  times larger than reported in *Dietrich et al.* [2010], and  $\approx 2.6$  times larger than other simultaneous microbursts observed by FIREBIRD-II [*Crew et al.*, 2016]. Lastly, the scale sizes derived here were similar to the scale sizes of  $> 15$  keV microbursts observed with a high altitude balloon [*Parks*, 1967]. No energy dependence on the scale size was observed.

The microburst scale size obtained in Section 3.3 and scaled to the geomagnetic equator can be compared with the scales of chorus waves presumably responsible for the rapid burst electron precipitation. Early direct estimates of the chorus source scales were made by the coordinated measurement by ISEE-1, 2. The wave power correlation scale was estimated to be about several hundred kilometers across the background magnetic field [*Gurnett et al.*, 1979]. Furthermore, *Santolik et al.* [2003] determined the correlation lengths of chorus-type whistler waves to be around 100 km based on multipoint CLUSTER Wide Band Data measurements near the chorus source region at  $L \approx 4$ , during the magnetic storm of 18 April 2002. *Agapitov et al.* [2010, 2011, 2017] recently showed that the spatial extent of chorus source region can be larger, ranging from 600 km in the outer radiation belt to more than 1000 km in the outer magnetosphere. The lower bound azimuthal and latitudinal scales obtained in Section 3.3 and scaled to the magnetic equator, are similar to the whistler-mode chorus source scale sizes reported in *Agapitov et al.* [2011, 2017].

No wave measurements from nearby spacecraft were available at this time. Nevertheless, during the hours before and after this observation, the Van Allen Probes' [*Mauk et al.*, 2013] Electric and Magnetic Field Instrument and Integrated Science [*Kletzing et al.*, 2013] observed strong wave power in the lower band chorus frequency range, inside the outer radiation belt between 22 and 2 MLT. Furthermore,  $AE \sim 400$  nT at this time, and relatively strong chorus waves were statistically more likely to be present at FIREBIRD-II's MLT [*Li et al.*, 2009].

The empirically estimated and modeled  $t_b$  in this study agree within FIREBIRD-II's uncertainties, confirming that the energy-dependent dispersion was due to bouncing. The  $t_b$  curves are a proxy for field line length, and this agreement implies that they are comparable. This is expected since the magnetosphere is not drastically compressed at 8 MLT, but we expect a larger discrepancy near midnight, where the magnetosphere is more stretched and more difficult to accurately model. This analysis can be used as a diagnostic tool to validate field line lengths in future studies.

The similarity of the microburst and chorus source region scale sizes, as well as magnetospheric location and conditions, further support the causal relationship between microbursts and chorus.



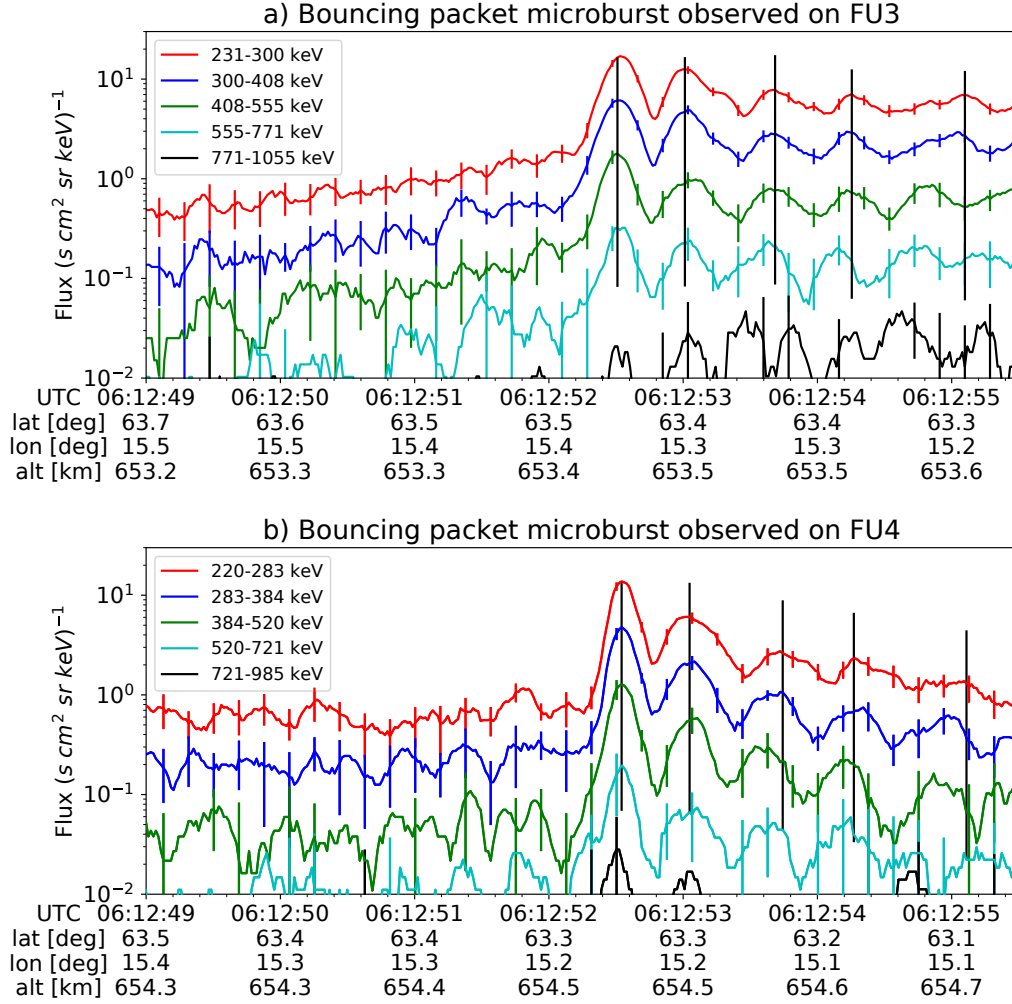


**Figure 1.** HiRes data of the microburst observed at February 2nd, 2015 at 06:12:53 UT, smoothed with a 150 ms rolling average. The subsequent bounces showed some energy dispersion. As discussed in the supporting information, a time correction of -2.28 s was applied to FU3. While the flux from five energy channels is shown, only channels with reasonable counting statistics were used for the spatial scale analysis. Vertical colored bars show the  $\sqrt{N}$  error every 10th data point and vertical black bars are lined up with the peaks in the 220-283 keV energy channel to help identify dispersion.

## Acknowledgments

This work was made possible with help from the FIREBIRD team, and the members of the Space Sciences and Engineering Laboratory at Montana State University for their hard work to make this mission a success. In addition, M. Shumko acknowledges Drew Turner for his suggestions regarding the bounce period calculations, and Dana Longcope for his proofreading feedback. The FIREBIRD-II data are available at [http://solar.physics.montana.edu/FIREBIRD\\_II/](http://solar.physics.montana.edu/FIREBIRD_II/). This analysis is supported by the National Science Foundation under Grant Numbers 0838034 and 1339414. Furthermore, the work of O. Agapitov was supported by the NASA grant NNX16AF85G.

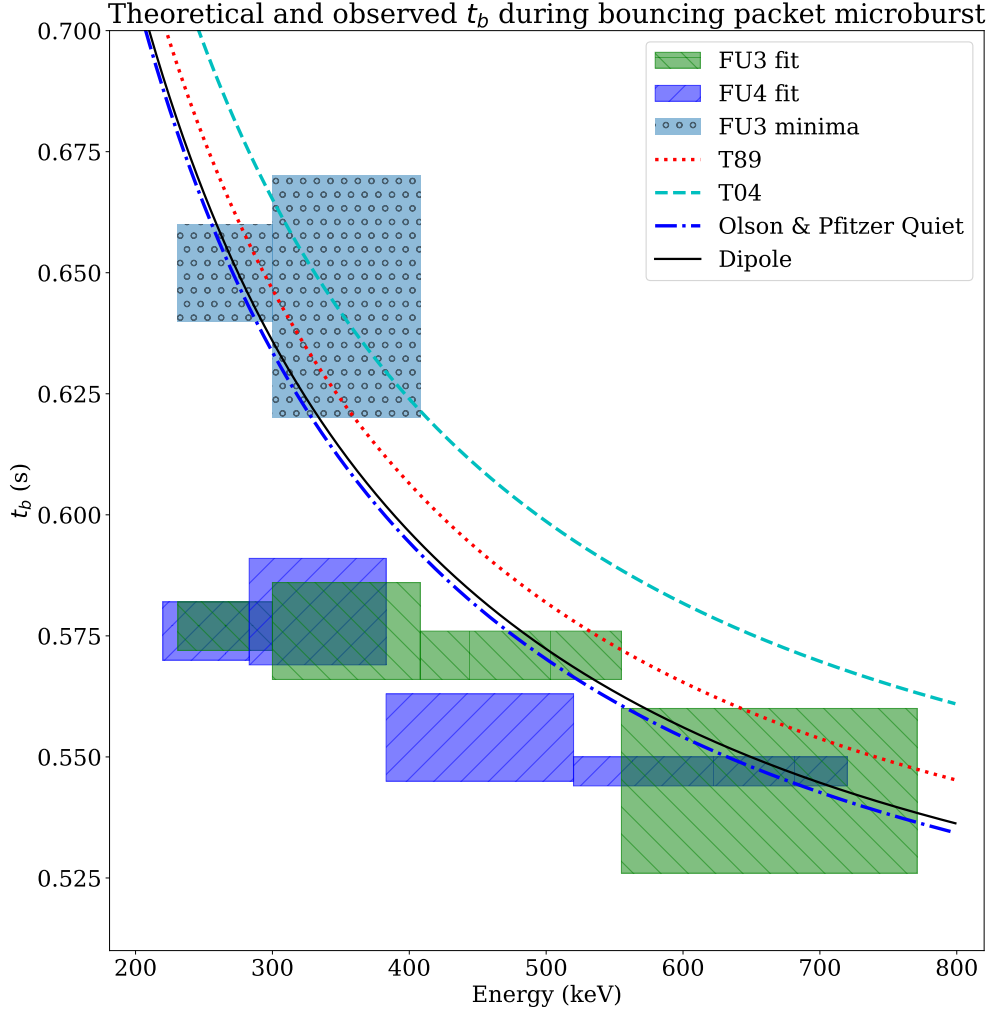


**Figure 2.** Observed and theoretical  $t_b$  for electrons of energies from 200 to 770 keV. The solid black line is  $t_b$  in a dipole magnetic field, derived in *Schulz and Lanzerotti* [1974]. The red and cyan dashed lines are the  $t_b$  derived using the T89, and T04 magnetic field models with IRBEM-Lib. Lastly, the blue dashed curve is the  $t_b$  derived using the Olson & Pfitzer Quiet model. The green and purple rectangles represent the observed  $t_b$  for FU3 and FU4 using a Gaussian fit, respectively. The blue rectangles represent the observed  $t_b$  calculated with the minima between the bounces. The width of the boxes represent the width of those energy channels, and the height represents the uncertainty from the fit.



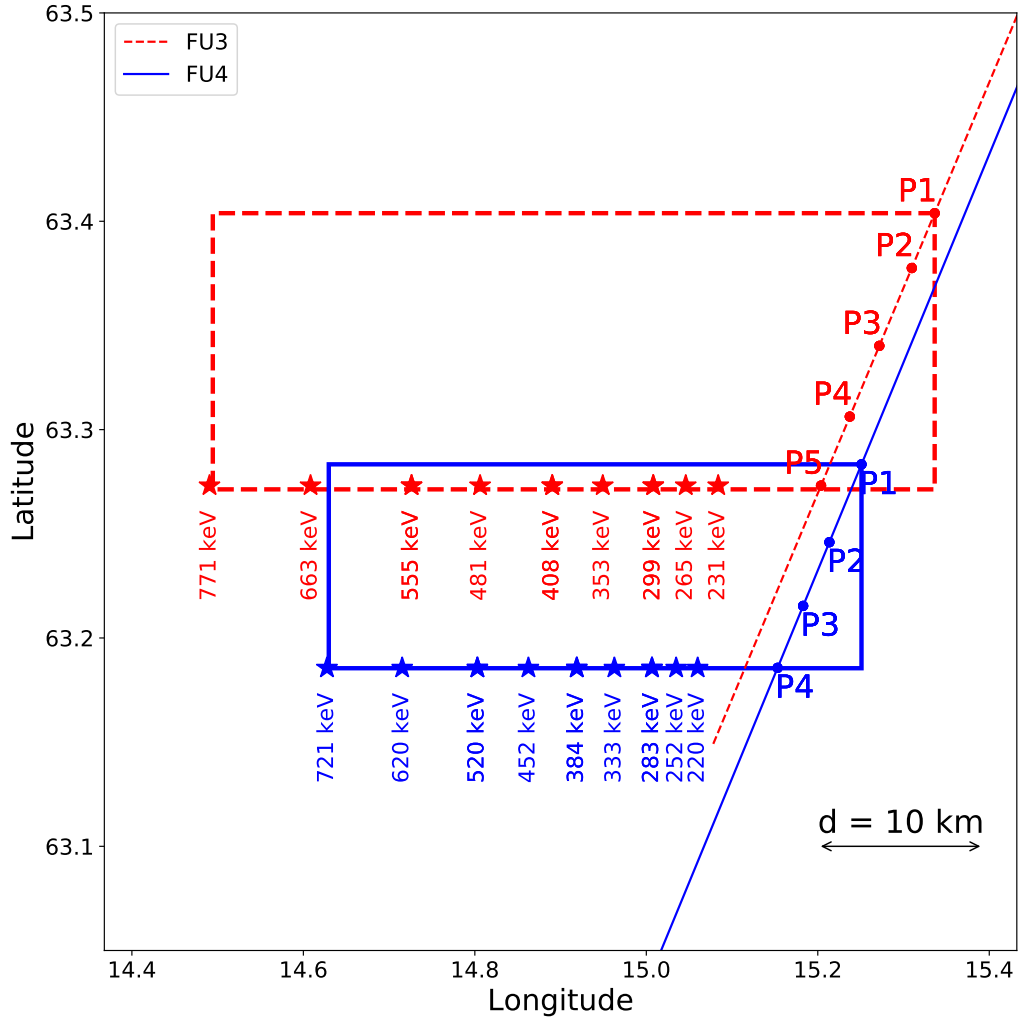


**Figure 3.** The topology of the FIREBIRD-II orbit and the multiple bounces of the microburst projected onto latitude and longitude with axis scaled to equal distance. Attributes relating to FU3 shown in red dashed lines, and FU4 with blue solid lines. The spacecraft path is shown with the diagonal lines, starting at the upper right corner. The labels P1-4 for FU4 and P1-5 for FU3 indicate where the spacecraft were when the  $N^{th}$  peak was seen in the lowest energy channel in the HiRes data. The stars with the accompanying energy labels represent the locations of the electrons with that energy that started at time of P1, and were seen at the last peak on each spacecraft. The rectangles represent the lower bound of the microburst scale size, assuming that the majority of the electrons were in the upper boundary of energy channel 4.

## References

- Abel, B., and R. M. Thorne (1998), Electron scattering loss in earth's inner magnetosphere: 1. dominant physical processes, *Journal of Geophysical Research: Space Physics*, 103(A2), 2385–2396.
- Agapitov, O., V. Krasnoselskikh, Y. Zaliznyak, V. Angelopoulos, O. Le Contel, and G. Rolland (2010), Chorus source region localization in the earth's outer magnetosphere using themis measurements, *Annales Geophysicae*, 28(6), 1377–1386, doi:10.5194/angeo-28-1377-2010.
- Agapitov, O., V. Krasnoselskikh, T. Dudok de Wit, Y. Khotyaintsev, J. S. Pickett, O. Santollik, and G. Rolland (2011), Multispacecraft observations of chorus emissions as a tool for the plasma density fluctuations' remote sensing, *Journal of Geophysical Research: Space Physics*, 116(A9), n/a–n/a, doi:10.1029/2011JA016540, a09222.
- Agapitov, O., L. W. Blum, F. S. Mozer, J. W. Bonnell, and J. Wygant (2017), Chorus whistler wave source scales as determined from multipoint van allen probe measurements, *Geophysical Research Letters*, pp. n/a–n/a, doi:10.1002/2017GL072701, 2017GL072701.
- Anderson, B., S. Shekhar, R. Millan, A. Crew, H. Spence, D. Klumpar, J. Blake, T. O'Brien, and D. Turner (2017), Spatial scale and duration of one microburst region on 13 august 2015, *Journal of Geophysical Research: Space Physics*.
- Anderson, K. A., and D. W. Milton (1964), Balloon observations of x rays in the auroral zone: 3. high time resolution studies, *Journal of Geophysical Research*, 69(21), 4457–4479, doi:10.1029/JZ069i021p04457.
- Blake, J., M. Looper, D. Baker, R. Nakamura, B. Klecker, and D. Hovestadt (1996), New high temporal and spatial resolution measurements by sampex of the precipitation of relativistic electrons, *Advances in Space Research*, 18(8), 171 – 186, doi: [http://dx.doi.org/10.1016/0273-1177\(95\)00969-8](http://dx.doi.org/10.1016/0273-1177(95)00969-8).
- Blum, L., X. Li, and M. Denton (2015), Rapid mev electron precipitation as observed by sampex/hilt during high-speed stream-driven storms, *Journal of Geophysical Research: Space Physics*, 120(5), 3783–3794, doi:10.1002/2014JA020633, 2014JA020633.
- Boscher, D., S. Bourdarie, P. O'Brien, T. Guild, and M. Shumko (2012), Irbem-lib library.
- Breneman, A., A. Crew, J. Sample, D. Klumpar, A. Johnson, O. Agapitov, M. Shumko, D. Turner, O. Santolik, J. Wygant, et al. (2017), Observations directly linking relativistic electron microbursts to whistler mode chorus: Van allen probes and firebird ii, *Geophysical Research Letters*.
- Crew, A. B., H. E. Spence, J. B. Blake, D. M. Klumpar, B. A. Larsen, T. P. O'Brien, S. Driscoll, M. Handley, J. Legere, S. Longworth, K. Mashburn, E. Mosleh, N. Ryhajlo, S. Smith, L. Springer, and M. Widholm (2016), First multipoint in situ observations of electron microbursts: Initial results from the nsf firebird ii mission, *Journal of Geophysical Research: Space Physics*, 121(6), 5272–5283, doi:10.1002/2016JA022485, 2016JA022485.
- Datta, S., R. Skoug, M. McCarthy, and G. Parks (1997), Modeling of microburst electron precipitation using pitch angle diffusion theory, *Journal of Geophysical Research: Space Physics*, 102(A8), 17,325–17,333.
- Dietrich, S., C. J. Rodger, M. A. Clilverd, J. Bortnik, and T. Raita (2010), Relativistic microburst storm characteristics: Combined satellite and ground-based observations, *Journal of Geophysical Research: Space Physics*, 115(A12).
- Fang, X., C. E. Randall, D. Lummerzheim, W. Wang, G. Lu, S. C. Solomon, and R. A. Frahm (2010), Parameterization of monoenergetic electron impact ionization, *Geophysical Research Letters*, 37(22).
- Gurnett, D., R. Anderson, F. Scarf, R. Fredricks, and E. Smith (1979), Initial results from the isee-1 and-2 plasma wave investigation, *Space Science Reviews*, 23(1), 103–122.
- Horne, R. B., and R. M. Thorne (2003), Relativistic electron acceleration and precipitation during resonant interactions with whistler-mode chorus, *Geophysical Research Letters*, 30(10), n/a–n/a, doi:10.1029/2003GL016973, 1527.

- Kletzing, C., W. Kurth, M. Acuna, R. MacDowall, R. Torbert, T. Averkamp, D. Bodet, S. Bounds, M. Chutter, J. Connerney, et al. (2013), The electric and magnetic field instrument suite and integrated science (emfisis) on rbsp, *Space Science Reviews*, 179(1-4), 127–181.
- Klumpar, D., L. Springer, E. Mosleh, K. Mashburn, S. Berardinelli, A. Gunderson, M. Handly, N. Ryhajlo, H. Spence, S. Smith, J. Legere, M. Widholm, S. Longworth, A. Crew, B. Larsen, J. Blake, and N. Walmsley (2015), Flight system technologies enabling the twin-cubesat firebird-ii scientific mission.
- Lee, J.-J., G. K. Parks, K. W. Min, H. J. Kim, J. Park, J. Hwang, M. P. McCarthy, E. Lee, K. S. Ryu, J. T. Lim, E. S. Sim, H. W. Lee, K. I. Kang, and H. Y. Park (2005), Energy spectra of 170–360 keV electron microbursts measured by the Korean STSAT-1, *Geophysical Research Letters*, 32(13), doi:10.1029/2005GL022996, 113106.
- Lee, J. J., G. K. Parks, E. Lee, B. T. Tsurutani, J. Hwang, K. S. Cho, K.-H. Kim, Y. D. Park, K. W. Min, and M. P. McCarthy (2012), Anisotropic pitch angle distribution of 100 keV microburst electrons in the loss cone: measurements from STSAT-1, *Annales Geophysicae*, 30(11), 1567–1573, doi:10.5194/angeo-30-1567-2012.
- Li, W., R. M. Thorne, V. Angelopoulos, J. Bortnik, C. M. Cully, B. Ni, O. LeContel, A. Roux, U. Auster, and W. Magnes (2009), Global distribution of whistler-mode chorus waves observed on the THEMIS spacecraft, *Geophysical Research Letters*, 36(9), n/a–n/a, doi:10.1029/2009GL037595, 109104.
- Lorentzen, K. R., J. B. Blake, U. S. Inan, and J. Bortnik (2001a), Observations of relativistic electron microbursts in association with VLF chorus, *Journal of Geophysical Research: Space Physics*, 106(A4), 6017–6027, doi:10.1029/2000JA003018.
- Lorentzen, K. R., M. D. Looper, and J. B. Blake (2001b), Relativistic electron microbursts during the geomagnetic storms, *Geophysical Research Letters*, 28(13), 2573–2576, doi:10.1029/2001GL012926.
- Mauk, B., N. J. Fox, S. Kanekal, R. Kessel, D. Sibeck, and A. Ukhorskiy (2013), Science objectives and rationale for the radiation belt storm probes mission, *Space Science Reviews*, 179(1-4), 3–27.
- Meredith, N., R. Horne, D. Summers, R. Thorne, R. Iles, D. Heynderickx, and R. Anderson (2002), Evidence for acceleration of outer zone electrons to relativistic energies by whistler mode chorus, in *Annales Geophysicae*, vol. 20, pp. 967–979.
- Millan, R., and R. Thorne (2007), Review of radiation belt relativistic electron losses, *Journal of Atmospheric and Solar-Terrestrial Physics*, 69(3), 362–377, doi: <http://dx.doi.org/10.1016/j.jastp.2006.06.019>, Global Aspects of Magnetosphere-Ionosphere Coupling.
- Millan, R. M., R. Lin, D. Smith, K. Lorentzen, and M. McCarthy (2002), X-ray observations of MeV electron precipitation with a balloon-borne germanium spectrometer, *Geophysical Research Letters*, 29(24).
- Mozer, F. S., O. V. Agapitov, J. B. Blake, and I. Y. Vasko (2018), Simultaneous observations of lower band chorus emissions at the equator and microburst precipitating electrons in the ionosphere, *Geophysical Research Letters*, pp. n/a–n/a, doi:10.1002/2017GL076120, 2017GL076120.
- Nakamura, R., D. N. Baker, J. B. Blake, S. Kanekal, B. Klecker, and D. Hovestadt (1995), Relativistic electron precipitation enhancements near the outer edge of the radiation belt, *Geophysical Research Letters*, 22(9), 1129–1132, doi:10.1029/95GL00378.
- Nakamura, R., M. Isowa, Y. Kamide, D. Baker, J. Blake, and M. Looper (2000), Observations of relativistic electron microbursts in association with VLF chorus, *J. Geophys. Res.*, 105, 15,875–15,885.
- O'Brien, T. P., K. R. Lorentzen, I. R. Mann, N. P. Meredith, J. B. Blake, J. F. Fennell, M. D. Looper, D. K. Milling, and R. R. Anderson (2003), Energization of relativistic electrons in the presence of ULF power and MeV microbursts: Evidence for dual ULF and VLF acceleration, *Journal of Geophysical Research: Space Physics*, 108(A8), n/a–n/a, doi:10.1029/2002JA009784, 1329.

- O'Brien, T. P., M. D. Looper, and J. B. Blake (2004), Quantification of relativistic electron microburst losses during the geomagnetic storms, *Geophysical Research Letters*, *31*(4), n/a–n/a, doi:10.1029/2003GL018621, 104802.
- Olson, W. P., and K. A. Pfizter (1982), A dynamic model of the magnetospheric magnetic and electric fields for July 29, 1977, *Journal of Geophysical Research: Space Physics*, *87*(A8), 5943–5948, doi:10.1029/JA087iA08p05943.
- Parks, G. (2003), *Physics Of Space Plasmas: An Introduction, Second Edition*, Westview Press.
- Parks, G. K. (1967), Spatial characteristics of auroral-zone x-ray microbursts, *Journal of Geophysical Research*, *72*(1), 215–226.
- Santolik, O., D. Gurnett, J. Pickett, M. Parrot, and N. Cornilleau-Wehrin (2003), Spatio-temporal structure of storm-time chorus, *Journal of Geophysical Research: Space Physics*, *108*(A7).
- Schulz, M., and L. J. Lanzerotti (1974), *Particle Diffusion in the Radiation Belts*, Springer.
- Selesnick, R. S., J. B. Blake, and R. A. Mewaldt (2003), Atmospheric losses of radiation belt electrons, *Journal of Geophysical Research: Space Physics*, *108*(A12), doi:10.1029/2003JA010160, 1468.
- Shprits, Y. Y., and R. M. Thorne (2004), Time dependent radial diffusion modeling of relativistic electrons with realistic loss rates, *Geophysical Research Letters*, *31*(8), n/a–n/a, doi:10.1029/2004GL019591, 108805.
- Shprits, Y. Y., N. P. Meredith, and R. M. Thorne (2007), Parameterization of radiation belt electron loss timescales due to interactions with chorus waves, *Geophysical Research Letters*, *34*(11), n/a–n/a, doi:10.1029/2006GL029050, 111110.
- Spence, H. E., J. B. Blake, A. B. Crew, S. Driscoll, D. M. Klumppar, B. A. Larsen, J. Legere, S. Longworth, E. Mosleh, T. P. O'Brien, S. Smith, L. Springer, and M. Widholm (2012), Focusing on size and energy dependence of electron microbursts from the van Allen radiation belts, *Space Weather*, *10*(11), doi:10.1029/2012SW000869.
- Summers, D., R. M. Thorne, and F. Xiao (1998), Relativistic theory of wave-particle resonant diffusion with application to electron acceleration in the magnetosphere, *Journal of Geophysical Research: Space Physics*, *103*(A9), 20,487–20,500.
- Thorne, R. M. (2010), Radiation belt dynamics: The importance of wave-particle interactions, *Geophysical Research Letters*, *37*(22), doi:10.1029/2010GL044990, 122107.
- Thorne, R. M., T. P. O'Brien, Y. Y. Shprits, D. Summers, and R. B. Horne (2005), Timescale for MeV electron microburst loss during geomagnetic storms, *Journal of Geophysical Research: Space Physics*, *110*(A9), n/a–n/a, doi:10.1029/2004JA010882, a09202.
- Tsyganenko, N. (1989), A solution of the Chapman-Ferraro problem for an ellipsoidal magnetopause, *Planetary and Space Science*, *37*(9), 1037 – 1046, doi: [http://dx.doi.org/10.1016/0032-0633\(89\)90076-7](http://dx.doi.org/10.1016/0032-0633(89)90076-7).
- Tsyganenko, N. A., and M. I. Sitnov (2005), Modeling the dynamics of the inner magnetosphere during strong geomagnetic storms, *Journal of Geophysical Research: Space Physics*, *110*(A3), n/a–n/a, doi:10.1029/2004JA010798, a03208.
- Ukhorskiy, A. Y., B. J. Anderson, P. C. Brandt, and N. A. Tsyganenko (2006), Storm time evolution of the outer radiation belt: Transport and losses, *Journal of Geophysical Research: Space Physics*, *111*(A11), n/a–n/a, doi:10.1029/2006JA011690, a11S03.
- Woodger, L., A. Halford, R. Millan, M. McCarthy, D. Smith, G. Bowers, J. Sample, B. Anderson, and X. Liang (2015), A summary of the barrel campaigns: Technique for studying electron precipitation, *Journal of Geophysical Research: Space Physics*, *120*(6), 4922–4935.